Journal of the Korean Physical Society, Vol. 72, No. 1, January 2018, pp. 38∼44

Epsilon-Near-Zero Enhanced Plasmonic Brewster Transmission Through Subwavelength Tapered Metallic Gratings

Phuc Toan Dang and Truong Khang Nguyen*
Division of Computational Physics, Institute for Computational Science, Ton Duc Thang University, Ho Chi Minh City, Vietnam and Faculty of Electrical & Electronics Engineering, Ton Duc Thang University, Ho Chi Minh City, Vietnam

Khai Quang Le
Division of Computational Physics, Institute for Computational Science, Ton Duc Thang University, Ho Chi Minh City, Vietnam

Tan Thi Pham
Faculty of Applied Sciences, University of Technology, Vietnam National University, Ho Chi Minh City, Vietnam

(Received 25 May 2017, in final form 16 August 2017)

Recently, epsilon-near-zero (ENZ) materials have been employed to stimulate light funnelling enhancement through a subwavelength metallic channel. In this paper, we present a study of enhanced optical transmission through subwavelength metallic gratings deposited on ENZ material and gallium-arsenide (GaAs) substrate. We propose to carve periodically tapered slits on the metallic grating to enable the impedance matching at the entrance and exit faces and thus enhance the light transmission at the plasmonic Brewster angle. The optimal grating geometry provides around 80% average transmission over a broad bandwidth from 5 THz to 20 THz at the incident Brewster angle of 76°. Our study extends potential practical applications of ENZ materials for integrated photonics.

PACS numbers: 41.20.Jb
Keywords: Epsilon-near-zero, Tapered gratings, Brewster angle, Transmission
DOI: 10.3938/jkps.72.38

I. INTRODUCTION

Next-generation photonics integrated circuit (PIC) research has been attempting to develop efficient methods for large-scale and high-dense integration of electronic and photonic components on a single chip. One of the basic demands for the realization of PICs is to effectively confine and guide light wave through subwavelength channels [1–4]. Guiding and confining light at subwavelength scales has faced many challenges due to the diffraction limit. Efforts to circumvent this problem have led to the introduction of artificial composite materials with fascinating plasmonic effects and metamaterial effects associated with anomalous permittivity and permeability having either negative or near-zero value [5, 6]. Among those, plasmonic gratings are special components which are able to guide light through subwavelength building blocks of the PICs. Particularly, building blocks in periodic systems such as subwavelength periodic metallic arrays enable extraordinary optical transmission (EOT) [7]. This anomalous transmission has attracted intensive research interest thanks to its potential applications in optical sensors, imaging, lithography, selective polarization filtering and energy concentrating [8–15]. The light transmission through the corrugated screen can be dramatically enhanced, in particular, for thinner apertures and larger periods owing to resonant modes such as surface plasmon resonances (SPRs), Fabry-Perot (FP) resonances on the metal film, or other resonant modes associated with the periodicity of the corrugations [16–23]. However, the EOT's bandwidth is inherently narrow, thus limits its applications, particular in light-emitting diodes. Efforts to broaden the bandwidth have led to the discovery of the plasmonic Brewster transmission [24]. The Brewster transmission is simply based on an inherently non-resonant mechanism. At a specific incidence angle, the Brewster angle, the total transverse-magnetic (TM)-polarized light transmission through the corrugated metal screen is achieved over

*E-mail: nguyentruongkhang@tdt.edu.vn

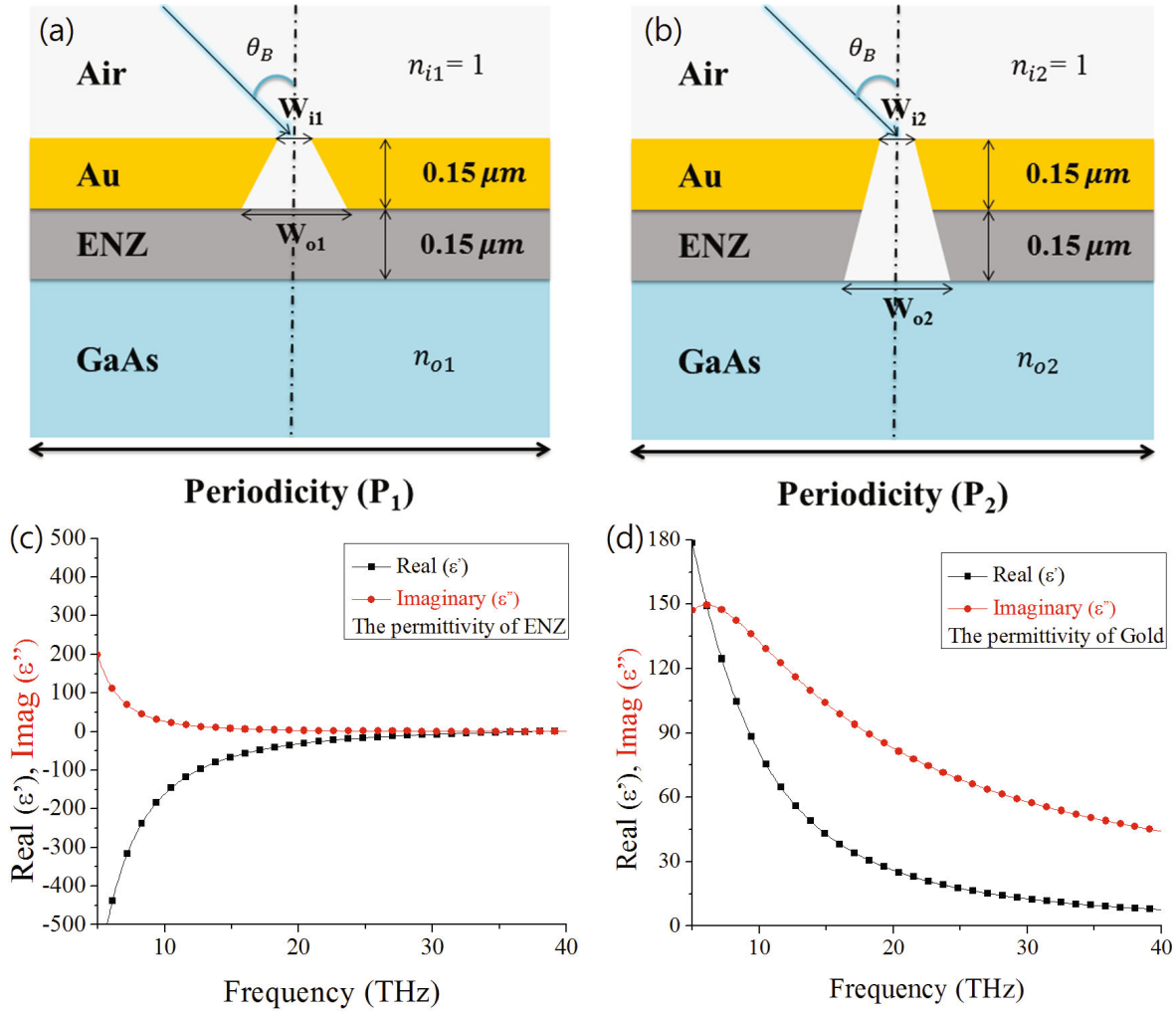

Fig. 1. (Color online) (a), (b) Schematic diagram of the two subwavelength slit structures used in the numerical calculations where the top and bottom layers are considered to be semi-infinite: (a) the ENZ based grating structure with a tapered slit carved through the Au layer only; (b) the GaAs based grating structure with a tapered slit carved through both the Au and ENZ layers. (c), (d) Dispersive properties of materials used in the structures: (c) ENZ material; (d) Au material.

a broad bandwidth owing to the impedance matching at the entrance and exit screen surfaces. This impedance matching can be achieved for mostly opaque screens. It is weakly dependent on the frequency and the screen thickness but selective to the incident angle.

Recently, a layer of epsilon-near-zero (ENZ) materials, which have tiny permittivity, has significantly provided possibilities for manipulating light through subwavelength objects [25,26]. Their properties have been also investigated in a channel waveguide based on a transmission-line model either with the tunnelling effects [27] or a thin slab by ENZ metamaterials which can be utilized to enhance the resolution of the optical system [28]. In particular, the ENZ material induces useful extraordinary optical properties such as near-zero refractive index inside the medium, enabling homogeneous distribution of electromagnetic fields and extending the local wavelength of light. In addition, ENZ materials can be manipulated to squeeze electromagnetic energy through narrow subwavelength waveguide channels, which reduces the reflection at a waveguide junction [29]. ENZ-enhanced transmission through a subwavelength channel was firstly demonstrated at optical (mid-infrared) frequencies in [30]. This paper reports a comprehensive research on ENZ materials for enhanced plasmonic Brewster transmission through a subwavelength metallic grating on a high-index substrate based on numerical solutions of Maxwell's equations.

It appears that as the metal screen is deposited on an ENZ material layer and a high-index gallium-arsenide (GaAs) substrate, the plasmonic Brewster transmission is significantly decreased due to the mismatch of impedance of epsilon-near-zero material and GaAs substrate with free space which leads to the impedance mismatch of the entrance and the exit face [31]. In this paper, we show that by adjusting the geometric sizes of

the metallic gratings and material properties, high transmission can be obtained over a broad bandwidth at the Brewster angle. The impedance matching concept can be applied to realize perfect broadband absorbers from the visible to IR regime [32,33] since we can manipulate the light/screen interaction to achieve no reflection at the entrance surface. It may also be applied to design anti-reflection coatings or reflection-type acoustic metasurfaces [34].

II. THEORY AND STRUCTURE MODELING

Extraordinary optical transmission through free-standing metallic gratings over a broad bandwidth from the visible to IR regime at the Brewster angle was demonstrated in [11,35,36]. In contrast to the conventional frequency selective surface (FSS) structures [37], these corrugated screens are much thicker and operate based on the impedance matching mechanism, supporting broadband transmission with no frequency selectivity at a specific angle of incidence. Considering the grating having thickness of l, width of w and periodicity of d, the reflection coefficient at the interface of the grating is given by TLM as

$$R = \frac{(Z_s^2 - Z_0^2)\tan(\beta_s l)}{(Z_s^2 + Z_0^2)\tan(\beta_s l) + 2iZ_sZ_0}, \quad (1)$$

where Z_s is the effective impedance of the slit, Z_0 is the characteristic impedance per unit length of the grating structure, and β_s is the slit wave number. From Eq. (1), zero reflection ($R = 0$) is achieved as either $\tan(\beta_s l) = 0$ or $Z_s = Z_0$ (Z_0 is a positive number). As the first condition is satisfied, $\beta_s l = n\pi$ with n being an integer, EOT with zero reflection happens at the usual FP resonance. As the second condition is met, the corrugated screen is anomalously impedance matched with free space as well as $Z_s = Z_0$. This condition is hardly met at normal incidence due to the opacity of metal but can be met by increasing the incidence angle θ so that at the specific angle satisfying

$$\cos\theta_B = (\beta_s w)/(k_0 d), \quad (2)$$

where θ_B is the plasmonic Brewster angle. The specific angle is independent of the grating thickness and operation frequency. At this angle, the impinging wave on the free-standing grating completely matches the effective slit impedance at the entrance and exit face resulting in total transmission through the grating [24]. It has been numerically and analytically demonstrated that in the transmission spectrum for the free-standing metascreen carved with straight slits, there exists a distinctive vertical band arising at the Brewster angle, θ_B, which showed very good agreement with the analytical formula (2). On the other hand, Eq. (2) is originated based on the impedance matching between the obliquely incident TM wave and the plasmonic mode supported inside the slit. Interestingly, such anomalous matching condition is totally independent of the grating thickness (l) but strongly dependent on the grating width (w) and the grating periodicity (d). Because the free-standing grating is impractical, the grating is typically deposited on a substrate, and thereby causing a significant decrease of Brewster transmission, particularly on a high-index substrate. For simplification purposes, we name the design with a tapered slit carved through the Au layer only as ENZ based grating structure (seen in Fig. 1(a)) and the design with a tapered slit carved through both the Au and ENZ layers as GaAs based grating structure (seen in Fig. 1(b)). Accordingly, the slit's width and the refractive index of the entrance and exit face of the gratings are denoted as (n_{i1}, W_{i1}) and (n_{o1}, W_{o1}) for the ENZ based grating structure, and (n_{i2}, W_{i2}) and (n_{02}, W_{o2}) for the GaAs based grating structure, respectively. The periodicities $P_1 = P_2 = 3$ μm, the ENZ's layer thickness $t_{ENZ} = 0.15$ μm, and the Au's layer thickness $t_{Au} = 0.15$ μm are same for both structures. To illustrate the effects of tapering in this structure, we assume the surrounding substrate and slit materials to be air. In the case of $n_i < n_o$, in order to allow impinging TM waves tunnelling and energy squeezing through the grating at the same Brewster angle, W_o should be larger than W_i [38]. In this study, the grating is deposited on a layer of ENZ materials with near-zero refractive index inside the medium and a GaAs substrate with refractive index of 3.3 in the THz regime. Therefore, n_{o1} is an effective refractive index which is an index combination of the ENZ layer and GaAs substrate. With the presence of ENZ material, it is expected to provide efficient coupling between free space radiation ($n_{i1} = 1$) and guiding light systems through the subwavelength tapered grating.

Figures 1(c) and (d) show the dispersive properties of the complex permittivity of the ENZ and Au materials in the frequency of interest 5 - 40 THz. The permittivity of the ENZ material was extracted from the experiment data [30] while that of the Au material was interpolated from the material library of CST [39]. All the simulation in this work is performed by the available electromagnetic simulation CST MICROWAVE STUDIO (CST MWS) package [39] in which the TM-polarized incident light on the grating is assumed as a plane wave with the angle of incidence θ. Moreover, total transmission over a broad bandwidth, arising exactly at the plasmonic Brewster angle, are calculated by Eq. (2).

III. RESULTS AND DISCUSSION

The impedance matching mechanism is lost when the grating is deposited on a high-index substrate causing a significant decrement in the plasmonic Brewster transmission [40,41]. We observe a horizontal band of about 60% transmission formed at 30 THz over a wide an-

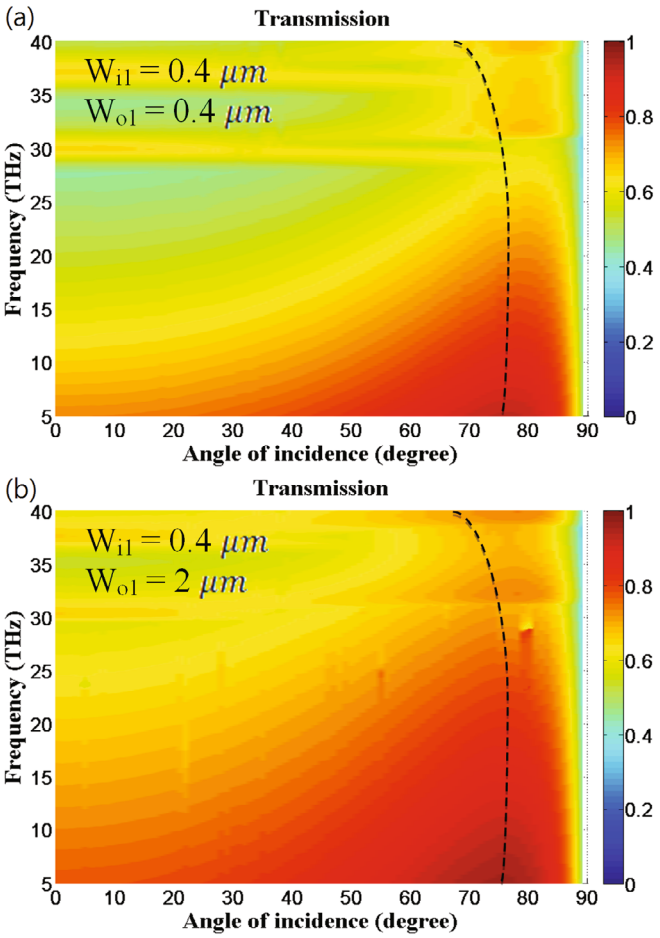

Fig. 2. (Color online) Angular transmission spectra as a function of frequency of the ENZ based grating structure; (a) for the straight slit with $W_{i1} = W_{o1} = 0.4$ μm, (b) for tapered slits with $W_{i1} = 0.4$ μm, $W_{o1} = 2$ μm. Both designs have the same Au thickness of 0.15 μm, ENZ thickness of 0.15 μm, and periodicity of 3 μm. The material between the slits of the structures is chosen to be free space $n_{o1} = 1$. The dashed lines indicate the predicted Brewster angle, given by Eq. (2).

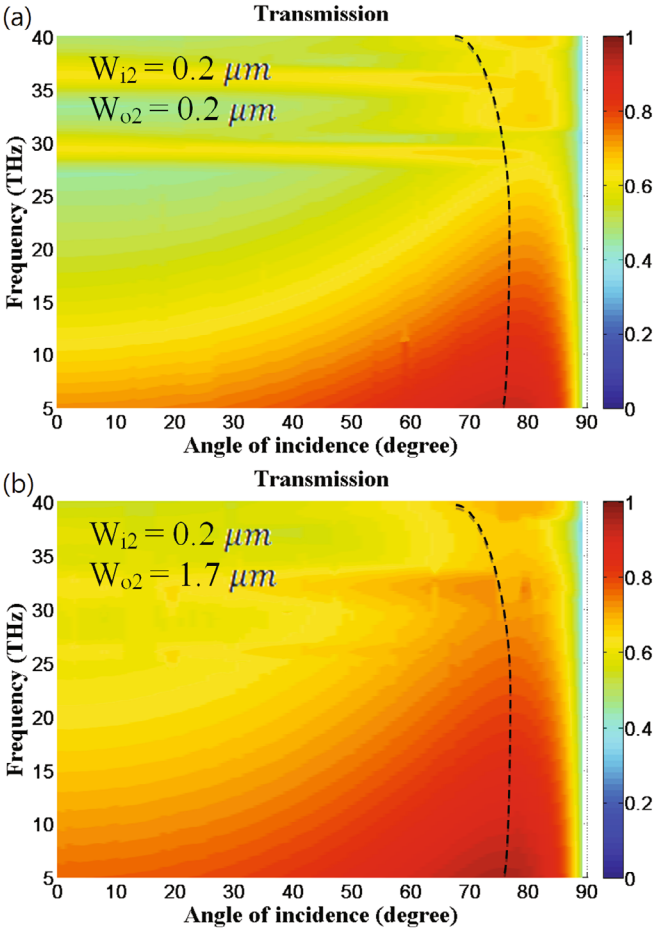

Fig. 3. (Color online) Similar to Fig. 2 but for the GaAs based grating structure; (a) for the straight slit with $W_{i2} = W_{o2} = 0.2$ μm; (b) for the tapered slit with $W_{i2} = 0.2$ μm, $W_{o2} = 1.7$ μm.

gle as shown in Fig. 2(a) with rectangular slit, *i.e.*, $W_{i1} = W_{o1} = 0.4$ μm, as a function of frequency and incident angle θ. This phenomenon is attributed to the excitation of FP resonance which is inherently narrowband in frequency but weakly dependent on the angle of incidence. However, at the plasmonic Brewster angle $\theta_B = 76°$, the transmission is remarkably decreased, in particular in 25 - 40 THz frequency range due to the high index contrast of the input (n_{i1})/output (n_{o1}) interface. To improve this plasmonic Brewster transmission, we add an intermediate layer of ENZ materials with realistic losses in the metallic grating to enhance light funnelling through this subwavelength channel. Moreover, we design and optimize the grating by carving periodically tapered slits in it as sketched in the ENZ based grating structure. It is found that the Brewster angle decreases as either the width of the slit or the refractive index of surrounding medium increases [34]. In order to attain the same Brewster angle with a given refractive index of the exit face, we adjust the slit's width of the exit face and the slit's width of the entrance face to enable its impedance matched with the surrounding medium [38]. Several simulations on the variations of slit widths (W_{i1} and W_{o1}) as well as grating period (P) are performed to find the optimum grating geometry to enable the impedance matching. Indeed, provided the grating depicted in the ENZ based grating structure having the thickness of $t_{g1} = t_{Au} = 0.15$ μm, the ENZ's thickness of $t_{ENZ} = 0.15$ μm, we found the highest Brewster transmission to be at $(P_1, W_{i1}, W_{o1}) = (3$ μm, 0.4 μm, 2 μm) with an average transmission of up to 80% over a broad range of 5 - 20 THz as seen in Fig. 2(b). The figure shows the simulated results that were carried out to determine optimal (P_1, W_{i1}, W_{o1}) of the ENZ based grating structure. Here P_1, W_{i1}, and W_{o1} were free variables in the simulation, and the average transmission was calculated as a ratio of the output and input power flows. In reality, as seen in Fig. 2(b) the Brewster transmis-

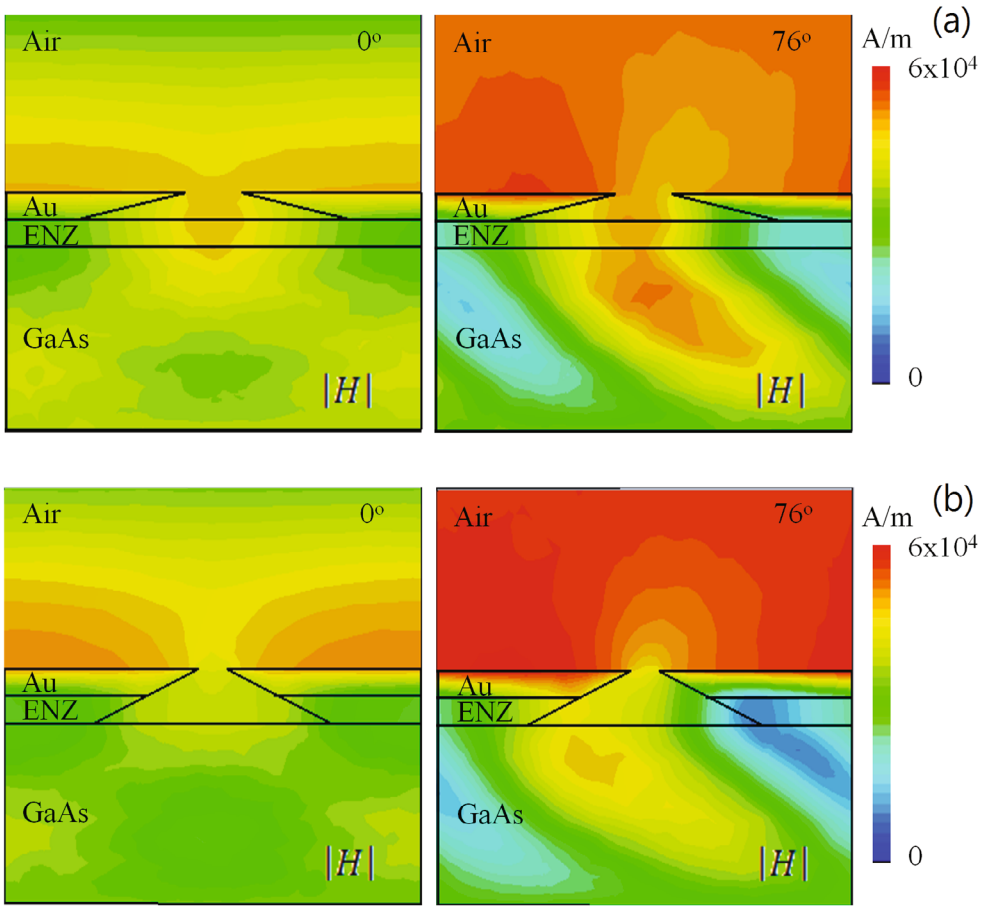

Fig. 4. (Color online) Comparison of absolute amplitude of magnetic fields at the particular frequency (f = 37.5 THz) at the normal incidence and plasmonic Brewster angle; (a) for the ENZ based grating structure; (b) for the GaAs based grating structure.

sion through the tapered slits with $W_{i1} < W_{o1}$ provides total transmission over a very broad bandwidth of frequency. It is obvious that the tapered grating provides higher transmission than that of the straight slits with $W_{i1} = W_{o1}$, particularly at oblique incidence.

Meanwhile, we also carried out to determine optimally (W_{i2}, W_{o2}) of the GaAs based grating structure with certain grating thickness of $t_{g2} = t_{Au} + t_{ENZ} = 0.3$ μm and periodicity of $P_2 = 3$ μm. Similar results were obtained as shown in Fig. 3. Figure 3(a) shows the light transmission effect through a rectangular slit which is periodically carved on the top GaAs substrate with $W_{i2} = W_{o2} = 0.2$ μm. The transmission in this case is based on the FP resonance mechanism which is retained at the normal incident ($\theta = 0°$). This resonance produces a horizontal transmission band near the 30 THz frequency but inherently limited in frequency. However, at the predicted Brewster angle $\theta_B = 76°$ a total transmission independent of the operation frequency through such straight slit was not as expected. A transmission of only about 60% was observed at this subwavelength transmission channel which is mainly caused by the high index contrast of the input/output interface ($n_{i2} = 1.0$ and $n_{02} = 3.3$). By tapering the slit, so this can be remedied thanks to the impedance adjustment at the slit's entrance and exit faces. We found that the average transmission of up to 76.5% is near $(W_{i2}, W_{o2}) = (0.2$ μm, 1.7 μm) in the 5 - 20 THz frequency range. Obviously, the tapered grating has greater performance than the rectangular grating for the light transmission structure of the TM polarization, particularly at the oblique incidence. In addition, the high width contrast of the input/output face $W_{o2}/W_{i2} = 8.5$ of the GaAs based grating structure is greater than the ratio of $W_{o1}/W_{i1} = 5$ in the ENZ based grating structure. This partly explains that the effective refractive index of the exit face in the ENZ based grating structure, *i.e.*, a composition of ENZ and GaAs, is slightly lower than that in the GaAs based grating structure.

The large transmission enhancement of the tapered grating-based structure may imply that the light is slowly squeezed from the entrance face onto the wider exit face. To highlight the anomalous features of light transmission phenomenon through the subwavelength gratings, we plot the magnetic field spatial distribution in the frequency range of operation from 20 to 40 THz for

the two gratings structures. Figure 4 shows the magnetic field amplitude at the frequency $f = 37.5$ THz, which represents the frequency of the plasmon resonance of the ENZ materials. In Fig. 4(a), we show the case of ENZ based grating structure, whereas in Fig. 4(b) we show the case of GaAs based grating structure at the normal incidence and plasmonic Brewster angle. Since the ENZ material is used as a coupling layer, the ENZ based grating structure shows stronger field intensity than that of the GaAs based grating structure. It is also seen that the field is strongly coupled and confined in the substrate in the ENZ based grating structure whereas the field tends to localize on the surface of the metallic grating in the GaAs counterpart. This behavior is more obvious at the Brewster's angle incident. At normal incidence, the transmission at FP resonance sets up a particularly standing wave propagation inside the slit. This FP channel is sensitive to the slit's geometry, the wavelength of light, and the existence of absorption along the slit. In contrast, at the Brewster channel, the plane wave propagates through the slit with nearly uniform amplitude and minimal reflection. The Brewster transmission is weakly dependent on the wavelength of light and the grating thickness.

Finally, we compare transmission spectra for the ENZ based grating structure and the GaAs based grating structure as a function of frequency at a normal incidence angle and plasmonic Brewster angle, shown in Fig. 5(a) and Fig. 5(b), respectively. In Fig. 5(a), we observe that the average transmission gradually increases with the angle, and reaches its maximum value of 80% at 76° area and 50.3% at normal incidence in 5 - 20 THz broadband range for the ENZ based grating structure. In Fig. 5(b), for the GaAs based grating structure, the average transmissions in 5 - 20 THz band obtained at normal incidence and Brewster angles are 48.4% and 76.5%, respectively. The presence of the ENZ layer increases the coupling efficiency of the incident light and consequently enhances the transmission of the ENZ based grating structure compared to that of the GaAs counterpart. Moreover, in order to accurately assess the role of the ENZ layer, we calculate average transmission in the extended frequency range of 5 - 40 THz. The average transmission at the Brewster's angle for the ENZ based grating structure reached over 63% while that of the GaAs counterpart was less than 62%. This increment is related to amplification of the amplitude of the field inside the ENZ material, as clearly seen in the 32 - 38 THz frequency range.

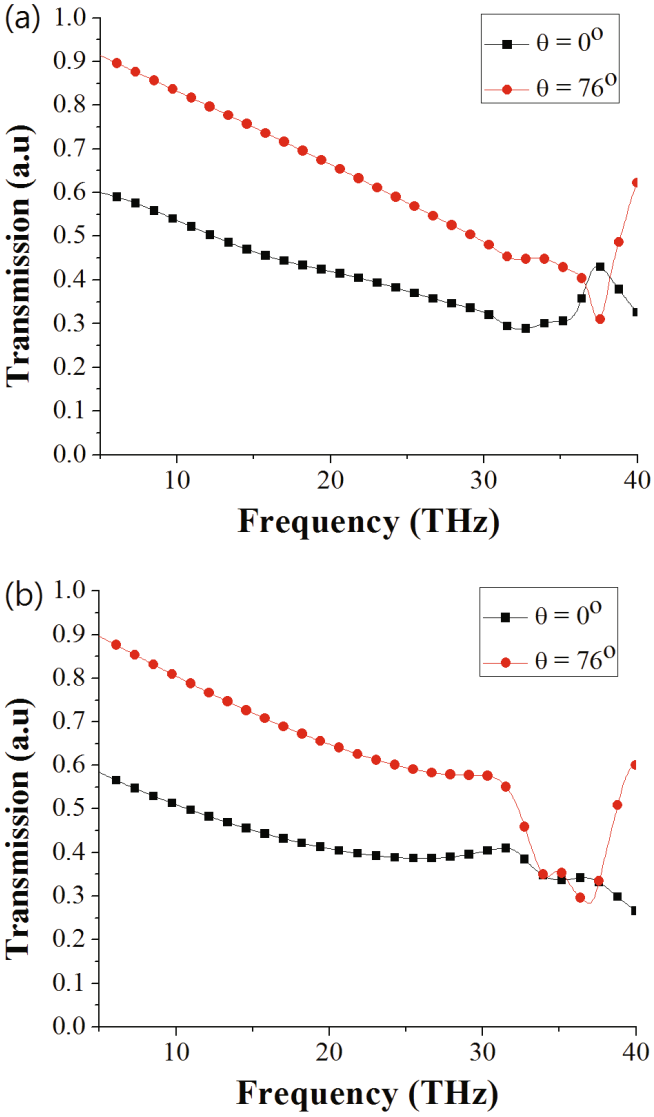

Fig. 5. (Color online) (a), (b) Transmission spectra as a function of frequency through the optimal tapered metallic gratings at the normal incidence angle (black-square line) and plasmonic Brewster angle (red-circular line): (a) the ENZ based grating structure; (b) the GaAs based grating structure.

IV. CONCLUSION

In this paper, we utilize a layer of ENZ materials with realistic losses to enhance light transmission through the subwavelength tapered metallic grating. We have optimized and tailored the metal grating carved periodically straight slits into tapered slits on a high-index substrate to enhance the extraordinary optical transmission in the THz regime. By gradually changing the slit width, we found that high average transmission up to 80% can be achieved over a broad bandwidth at the Brewster angle. We have explored the concept of the ENZ material enhanced plasmonic Brewster transmission to closer to practical applications since its substrate influence, and realistic losses materials were taken into account.

ACKNOWLEDGMENTS

This research is funded by Vietnam National Foundation for Science and Technology Development (NAFOSTED) under grant number "103.03-2017.32".

REFERENCES

[1] R. Zia, J. A Schuller, A. Chandran and M. L. Brongersma, Mater. Today. **9**, 20 (2006).
[2] D. J. Lockwood and L. Pavesi, *Silicon photonics* (Heidelberger, Berlin, 2004).
[3] D. K. Gramotnev and S. I. Bozhevolnyi, Nature. Photonics. **4**, 83 (2010).
[4] W. L. Barnes, A. Dereux and T. W. Ebbesen, Nature. **424**, 824 (2003).
[5] M. Stepanova and S. Dew, *Nanofabrication: Techniques and Principles* (Springer Wien, New York, 2012).
[6] M. A. Noginov and V. A. Podolskiy, *Tutorials in Metamaterials* (Boca Raton, FL, 2012).
[7] T. W. Ebbesen, H. J. Lezec, H. F. Ghaemi, T. Thio and P. A. Wolff, Nature. **391**, 667 (1998).
[8] F. J. Garcia-Vidal, L. Martin-Moreno, T. W. Ebbesen and L. Kuipers, Rev. Mod. Phys. **82**, 729 (2010).
[9] A. De Leebeeck, L. K. S. Kumar, V. de Lange, D. Sinton, R. Gordon and A. G. Brolo, Anal. Chem. **79**, 4094 (2007).
[10] R. Gordon, D. Sinton, K. L. Kavanagh and A. G. Brolo, Acc. Chem. Res. **41**, 1049 (2008).
[11] J. Choi, K. Kim, Y. Oh, A. L. Kim, S. Y. Kim, J. Shin and D. Kim, Adv. Opt. Matter. **2**, 48 (2013).
[12] L. Neumann, Y. Pang, A. Houyou, M. L. Juan, R. Gordon and N. F. van Hulst, Nano Lett. **11**, 355 (2011).
[13] R. Ortuño, C. García-Meca, F. J. Rodríguez-Fortuño, A. Håkansson, A. Griol, J. Hurtado, J. A. Ayucar, L. Bellieres, P. J. Rodríguez, F. López-Royo, J. Martí and A. Martínez, J. App. Phys. **106**, 124313 (2009).
[14] J. S. White, G. Veronis, Z. Yu, E. S. Barnard, A. Chandran, S. Fan and M. L. Brongersma, Opt Lett. **34**, 686 (2009).
[15] S. Saxena, R. P. Chaudhary, A. Singh, S. Awasthi and S. Shukla, Sci. Rep. **4**, 5586 (2014).
[16] H. Liu and P. Lalanne, Nature. **452**, 728 (2008).
[17] L. Martín-Moreno, F. J. García-Vidal, H. J. Lezec, K. M. Pellerin, T. Thio, J. B. Pendry and T. W. Ebbesen, Phys. Rev. Lett. **86**, 1114 (2001).
[18] F. J. García de Abajo, R. Gómez-Medina and J. J. Sáenz, Phys. Rev. E **72**, 016608 (2005).
[19] V. Delgado, R. Marqués and L. Jelinek, Opt. Express **18**, 6506 (2010).
[20] X-R. Huang, R-W. Peng and R-H. Fan, Phys. Rev. Lett. **105**, 243901 (2010).
[21] F. Van Beijnum, C. Rétif, C. B. Smiet, H. Liu, P. Lalanne, M. P. van Exter, Nature. **492**, 411 (2012).
[22] W. Wen, L. Zhou, B. Hou, C. T. Chan and P. Sheng, Phys. Rev. B **72**, 153406 (2005).
[23] B. Hou, Z. H. Hang, W. Wen, C. T. Chan and P. Sheng, Appl. Phys. Lett. **89**, 131917 (2006).
[24] A. Alù, G. D'Aguanno, N. Mattiucci and M. J. Bloemer, Phys. Rev. Lett. **106**, 123902 (2011).
[25] R. W. Ziolkowski, Phys. Rev. E **70**, 046608 (2004).
[26] A. Alù, M. G. Silveirinha, A. Salandrino and N. Engheta, Phys. Rev. B **75**, 155410 (2007).
[27] B-M. Kim, H-W. Son, Y-K. Cho and J-P. Hong, J. Korean Phys. Soc. **65**, 625 (2014).
[28] Y-R. Jang, S. B. Choi, D. J. Park and J. Kyoung, J. Korean Phys. Soc. **69**, 268 (2016).
[29] M. G. Silveirinha and N. Engheta, Phys. Rev. Lett. **97**, 157403 (2006).
[30] D. C. Adams, S. Inampudi, T. Ribaudo, D. Slocum, S. Vangala, N. A. Kuhta, W. D. Goodhue, V. A. Podolskiy and D. Wasserman, Phys. Rev. Lett. **107**, 133901 (2011).
[31] C. Argyropoulos, G. D'Aguanno, N. Mattiucci, N. Akozbek, M. J. Bloemer and A. Alù, Phys. Rev. B **85**, 024304 (2012).
[32] C. Argyropoulos, K. Q. Le, N. Mattiucci, G. D'Aguanno and A. Alù, Phys. Rev. B **87**, 205112 (2013).
[33] N. Mattiucci, M. J. Bloemer, N. Aközbek and G. D'Aguanno, Sci. Rep. **3**, 3203 (2013).
[34] J. Mei and Y. Wu, New. J. Phys. **16**, 123007 (2014).
[35] K. Q. Le, C. Argyropoulos, N. Mattiucci, G. D'Aguanno, M. J. Bloemer and A. Alù, J. Appl. Phys. **112**, 094317 (2012).
[36] K. Q. Le, C. Argyropoulos and A. Alù, Proc. SPIE. **8423**, 842313 (2012).
[37] D. Van Labeke, D. Gérard, B. Guizal, F. I. Baida and L. Li, Opt. Express. **14**, 11945 (2006).
[38] K. Q. Le, J. Appl. Phys. **115**, 033110 (2014).
[39] *CST GmbH* (2016) CST Microwave Studio. http://www.cst.com
[40] T. K. Nguyen, K. Q. Le and I. Park, *IEEE International Symposium on Antennas and Propagation (APS/URSI)* (2016), p. 23.
[41] T. K. Nguyen, P. T. Dang, I. Park and K. Q. Le, J. Opt. Soc. Am. B **34**, 583 (2017).